The Journal of Immunology

Anti–PD-1 Antibody Treatment Promotes Clearance of Persistent Cryptococcal Lung Infection in Mice

Jonathan A. Roussey, Steven P. Viglianti, Seagal Teitz-Tennenbaum, Michal A. Olszewski and John J. Osterholzer

J Immunol 2017; 199:3535-3546; Prepublished online 16 October 2017;
doi: 10.4049/jimmunol.1700840
http://www.jimmunol.org/content/199/10/3535

The Journal of Immunology is published twice each month by
The American Association of Immunologists, Inc.,
1451 Rockville Pike, Suite 650, Rockville, MD 20852

Print ISSN: 0022-1767 Online ISSN: 1550-6606.

Anti–PD-1 Antibody Treatment Promotes Clearance of Persistent Cryptococcal Lung Infection in Mice

Jonathan A. Roussey,*,† Steven P. Viglianti,* Seagal Teitz-Tennenbaum,*,† Michal A. Olszewski,*,†,‡ and John J. Osterholzer†,‡,§

Activation of immunomodulatory pathways in response to invasive fungi can impair clearance and promote persistent infections. The programmed cell death protein-1 (PD-1) signaling pathway inhibits immune effector responses against tumors, and immune checkpoint inhibitors that block this pathway are being increasingly used as cancer therapy. The objective of this study was to investigate whether this pathway contributes to persistent fungal infection and to determine whether anti–PD-1 Ab treatment improves fungal clearance. Studies were performed using C57BL/6 mice infected with a moderately virulent strain of *Cryptococcus neoformans* (52D), which resulted in prolonged elevations in fungal burden and histopathologic evidence of chronic lung inflammation. Persistent infection was associated with increased and sustained expression of PD-1 on lung lymphocytes, including a mixed population of $CD4^+$ T cells. In parallel, expression of the PD-1 ligands, PD-1 ligands 1 and 2, was similarly upregulated on specific subsets of resident and recruited lung dendritic cells and macrophages. Treatment of persistently infected mice for 4 wk by repetitive administration of neutralizing anti–PD-1 Ab significantly improved pulmonary fungal clearance. Treatment was well tolerated without evidence of morbidity. Immunophenotyping revealed that anti–PD-1 Ab treatment did not alter immune effector cell numbers or myeloid cell activation. Treatment did reduce gene expression of IL-5 and IL-10 by lung leukocytes and promoted sustained upregulation of OX40 by Th1 and Th17 cells. Collectively, this study demonstrates that PD-1 signaling promotes persistent cryptococcal lung infection and identifies this pathway as a potential target for novel immune-based treatments of chronic fungal disease. ***The Journal of Immunology*****, 2017, 199: 3535–3546.**

Cryptococcus neoformans is an encapsulated fungus acquired by inhalation. Pulmonary infection with *C. neoformans* results in one of three generalized outcomes: clearance, persistence, or progression (1). Persistent and progressive infections are frequent in immunocompromised individuals; infection with *C. neoformans* constitutes the second most common fungal infection in organ transplant recipients (1). Further, out of an estimated 278,000 new cases of cryptococcosis annually, ∼223,100 patients will develop cryptococcal meningitis, with 81% of these cases resulting in death (2); thus, cryptococcal disease is the second leading cause of AIDS-related mortality in HIV^+ individuals behind tuberculosis. In patients surviving initial infection, up to 15% of HIV^+, *C. neoformans*–infected individuals relapse despite conventional antifungal treatments (3). Although uncommon, clinically significant infections have been reported in seemingly immunocompetent hosts (4–6). Antibiotic treatment of these infections is often toxic and lengthy (potentially lifelong) (7). Thus, novel approaches that augment conventional therapy are needed.

Persistent cryptococcal lung infection, effectively modeled by intratracheal inoculation of C57BL/6 mice with a moderately virulent strain of *C. neoformans* (52D), is characterized by a mixed Th polarization immunophenotype, which contains but does not eliminate the fungus (8–12). Persistent lung infection reflects an immune balance between concurrent induction of IFN-γ and IL-17, which promote classical (M1) macrophage activation and fungal killing (13–16), with expression of IL-4, IL-13, and IL-10, which promote alternative (M2) macrophage activation and intracellular fungal survival (9, 15, 17). Our studies have shown that *C. neoformans* can evade host defenses by expression of virulence factors that impair type 1 (T1) and favor nonprotective type 2 (T2) responses (18–20). To counteract this, we have successfully intervened with anti–IL-10R Ab blockade, which augmented protective T1 immunity and improved fungal clearance in persistently infected mice (17). Importantly, these studies demonstrated that exogenous immune modulation, even at late stages of established infection, can be therapeutically effective.

In this study, we investigate whether the programmed cell death protein-1 (PD-1) pathway contributes to persistent cryptococcal lung infection. PD-1 and its two ligands, PD-1 ligand-1 (PD-L1) and PD-1 ligand 2 (PD-L2), comprise an important immunomodulatory pathway that under homeostatic conditions limits effector immune responses and promotes tolerance (reviewed in Ref. 21).

*Research Service, Ann Arbor Veterans Affairs Health System, Department of Veterans Affairs Health System, University of Michigan Health System, Ann Arbor, MI 48103; †Division of Pulmonary and Critical Care Medicine, Department of Internal Medicine, University of Michigan Health System, Ann Arbor, MI 48103; ‡Graduate Program in Immunology, University of Michigan Health System, Ann Arbor, MI 48103; and §Pulmonary Section, Medical Service, University of Michigan Health System, Ann Arbor, MI 48103

ORCID: 0000-0001-7474-0843 (M.A.O.).

Received for publication June 12, 2017. Accepted for publication September 18, 2017.

This work was supported by a Merit Review Award (to J.J.O.) from the Biomedical Laboratory Research and Development Service, the Department of Veterans Affairs, and a National Institutes of Health T32 Training Grant (to J.A.R., trainee).

Portions of this work were presented at the International Conference of the American Thoracic Society, May 23, 2017, Washington, DC.

Address correspondence and reprint requests to Dr. John J. Osterholzer, University of Michigan/Ann Arbor Veterans Affairs Medical Center, Pulmonary and Critical Care Medicine Section (111G), Department of Veterans Affairs Hospital, 2215 Fuller Road, Ann Arbor, MI 48105-2303. E-mail address: oster@umich.edu

The online version of this article contains supplemental material.

Abbreviations used in this article: AM, alveolar macrophage; cDC, conventional DC; Cy, cyanine; DC, dendritic cell; ExM, exudate macrophage; iNOS, inducible NO synthase; moDC, monocyte-derived DC; PD-1, programmed cell death protein-1; PD-L1, PD-1 ligand 1; PD-L2, PD-1 ligand 2; qPCR, quantitative RT-PCR; T1, type 1; T2, type 2; Treg, T regulatory; WOT, wk of treatment; WPI, wk postinfection.

PD-1 is primarily expressed on lymphoid cells, especially activated T cells (22, 23). PD-L1 is expressed on a wide variety of APCs, T cells, and epithelial cells, whereas PD-L2 expression is restricted primarily to APCs (22). Our interest in studying this pathway in the context of fungal persistence stems from studies demonstrating that PD-1 signaling impairs clearance of some viral (24–26) and bacterial pathogens (27, 28). Furthermore, numerous studies have shown that this pathway promotes tumor immune evasion, which has led to the development of potent immune checkpoint inhibitors that effectively treat tumors in mice (29, 30) and humans (reviewed in Refs. 31, 32).

Knowledge of the role of this pathway in cryptococcal infection is limited. A study by Guerrero et al. (33) demonstrated that infection with more virulent, mucoid colonies of *C. neoformans* is associated with increased expression of PD-L1 and PD-L2 by alveolar macrophages (AMs). We have recently showed that GM-CSF promotes PD-L2 expression by dendritic cells (DCs) in the lungs of mice with persistent cryptococcal lung infection (8). Neither study provided a detailed evaluation of this pathway throughout infection or assessed the therapeutic effects of PD-1 blockade. Results of this study show that persistent cryptococcal lung infection induced broad and sustained upregulation of PD-1 and its ligands, PD-L1 and PD-L2, on specific lung lymphoid and myeloid cell subsets. Treatment of persistently infected mice with a blocking anti–PD-1 Ab enhanced fungal clearance, likely through mechanisms that diminished T2 bias and enhanced T cell activation. Collectively, this study demonstrates that the PD-1 signaling pathway promotes persistent cryptococcal lung infection, and that targeted blockade of this pathway is therapeutically beneficial and well tolerated.

Materials and Methods

Mice

Female C57BL/6J mice were obtained from The Jackson Laboratory (Bar Harbor, ME) and housed under specific pathogen-free conditions in the Animal Care Facility at the VA Ann Arbor Healthcare System. All experiments were approved by the Veterans Administration Institutional Animal Care and Use Committee. Mice were 8–12 wk of age at the time of infection with *C. neoformans*.

C. neoformans

C. neoformans strain 52D was obtained from the American Type Culture Collection (catalog no. 24067; Manassas, VA) and grown to a late logarithmic phase by incubation on a shaker at 37˚C for 60–72 h in Sabouraud dextrose broth (1% Neopeptone, 2% dextrose; Difco, Detroit, MI). Cultures were centrifuged and the pellets washed with nonpyrogenic saline (Travenol, Deerfield, IL). Cells were counted in the presence of trypan blue using a hemocytometer and subsequently resuspended at 3.33×10^5 cells/ml in nonpyrogenic saline immediately before intratracheal inoculation.

Intratracheal inoculation of C. neoformans

Mice were anesthetized by i.p. injection of ketamine (100 mg/kg; Hospira, Lake Forest, IL) and xylazine (6.8 mg/kg; Lloyd Laboratories, Shenandoah, IA). Following a midline neck incision, strap muscles were separated laterally to expose the trachea. Under direct vision, 10^4 *C. neoformans* (suspended in 30 μl of nonpyrogenic saline) were injected into the trachea using a 30-gauge needle attached to a 1-ml syringe mounted on a repetitive pipette (Stepper; Tridak, Brookfield, CT). After inoculation, skin was closed using a cyanoacrylate adhesive.

Tissue collection

Lungs were perfused in situ via the right ventricle using 8–10 ml of PBS until pulmonary vessels appeared clear. Lungs were excised, minced, and placed in a gentleMACS C tube (Miltenyi Biotec, San Diego, CA) containing 5 ml of digestion buffer (34). After a short, gentle agitation using a gentleMACS dissociator (Miltenyi Biotec), lung suspensions were incubated on a rotator at 37˚C for 35 m. Lung suspensions were next vigorously homogenized using a gentleMACS dissociator and centrifuged. ACK lysing buffer (KD Medical, Columbia, MD) was used to lyse erythrocytes. Samples were then passed through 10-ml syringes rapidly 10–12 times to further break apart tissue and cell clumps. Next, samples were centrifuged in 20% Percoll gradients (Sigma-Aldrich, St. Louis, MO) to separate leukocytes from epithelial cells and debris. Thereafter, cells were resuspended in RPMI 1640 complete media (34) and counted on a hemocytometer in the presence of trypan blue.

RNA isolation and quantitative RT-PCR

Five million cells were pelleted in 1.5-ml microcentrifuge tubes, and RNA was isolated using TRIzol (Ambion, Life Technologies, Carlsbad, CA). DNA contamination was removed using the Turbo DNA-free kit (Ambion, Life Technologies) according to the manufacturer's instructions. RNA was quantified and assessed for quality using a NanoDrop 2000 (Thermo Fisher Scientific, Wilmington, DE). Quantitative RT-PCR (qRT-PCR) was performed using the QuantiTect SYBR Green RT-PCR Kit (Qiagen, Germantown, MD) according to the manufacturer's instructions with a StepOnePlus Real-Time PCR System (Thermo Fisher Scientific). qRT-PCR primers are listed in Supplemental Table I.

PD-1 blocking Ab

A low-endotoxin (<2 endotoxin units/mg), azide-free, purified Ab against murine PD-1 (clone RMP1-14) or rat IgG2a, κ low-endotoxin isotype control Ab (clone 2A3) (both from Bio X Cell, West Lebanon, NH) was administered at a dose of 200 μg of Ab in 200 μl of sterile PBS (~10 mg/kg) via i.p. injection twice per wk based on the previously established efficacy of this dosing strategy in other experimental models of fungal infection (35, 36). Treatment was initiated at 3 wk postinfection (WPI) and continued for either 2 or 4 wk.

CFU assay

To assess fungal burden, we plated 10-μl aliquots of lung digests or brain or spleen homogenates on Sabouraud dextrose agar plates in duplicate serial 10-fold dilutions. Plates were incubated at room temperature for 45–48 h. At the end of incubation, colonies were counted and CFUs per organ was calculated.

Effect of isotype control and anti–PD-1 Abs on fungal growth in vitro

To assess the effect of Abs on the growth of *C. neoformans* in vitro, we cultured 10^6 *C. neoformans* in Sabouraud dextrose broth media at 37˚C with either 0.8 (low) or 8.0 μg/ml (high) anti–PD-1 or rat IgG2a isotype control Ab followed by counting viable *C. neoformans* on a hemocytometer at 24 and 48 h.

Lung histology

Lungs were fixed by inflation with a 1:1 mixture of PBS and Optimum Cutting Temperature compound followed by freezing on dry ice. After freezing, 5-μm sections were cut and stained with H&E for histological analysis.

Abs for flow cytometry

Abs targeting the following murine proteins were purchased from BioLegend (San Diego, CA): PD-L1 (clone 10F.9G2), I-A/I-E (M5/114.15.2), CD45 (30-F11), CD19 (6D5), CD11b (M1/70), PD-1 (29F.1A12), TCRβ-chain (H57-597), CD8a (53-6.7), PD-L2 (TY25), CD80 (16-10A1), CD4 (GK1.5), Ly6G (1A8), Ly6C (HK1.4), T-bet (4B10), ICOS (C398.4A), OX40 (OX-86), TCRγ/δ (GL3), and CD16/32 (clone 93). Abs targeting the following murine proteins were purchased from BD Biosciences (Franklin Lake, NJ): Siglec F (E50-2440), CD24 (M1/69), and CD3ε (145-2C11). Abs targeting the following murine proteins were purchased from eBioscience (Ashville, NC): inducible NO synthase (iNOS; CXNFT), Foxp3 (FJK-16s), Ki67 (SolA15), CD11c (N418), Gata3 (TWAJ), and *Rorγt* (B2D). A polyclonal Ab targeting murine arginase was purchased from R&D Systems. Isotype control Abs were used according to manufacturer's instructions in all experiments. Abs were conjugated to the following fluorophores: allophycocyanin, Alexa Fluor 700, allophycocyanin-cyanine (Cy) 7, FITC, PE, PerCP-Cy5.5, PE-eFluor 610, PE-Cy5, PE-Cy7, brilliant violet 421, and brilliant violet 650.

Cell staining and flow cytometry

Cell surface staining, including blockade of Fc receptors, and sample analysis by flow cytometry were performed as described previously (34). For staining of intracellular and nuclear proteins, cells were incubated with a viability dye (Zombie Aqua Fixable Viability dye; BioLegend) for 20 min at room temperature in the dark. Cells were next washed in PBS, then

incubated with an Fc receptor–blocking Ab for 10 min at 4°C. After washing, cells were incubated and washed using a transcription factor staining kit (Foxp3/transcription factor staining kit; eBioscience) per manufacturer's instructions. Thereafter, cells were incubated with Abs raised against cytoplasmic and nuclear Ags (in permeabilization buffer) for 30 min at room temperature in the dark. Cells were then washed twice with permeabilization buffer and subsequently stored in 2% paraformaldehyde in PBS overnight. Flow cytometry was performed on either a Becton Dickinson (BD) LSR II or a BD LSR Fortessa (BD Biosciences), utilizing 12 detector channels. After gating out debris and doublets, a total of 100,000 events was acquired from each sample using FACSDiva data acquisition software. Data were analyzed using FlowJo software (Tree Star, Ashland, OR). Specific leukocyte populations were identified using gating strategies described in the *Results* and the figure legends. To calculate the total number of cells in each population of interest in each sample, we multiplied the corresponding percentage by the total number of $CD45^+$ cells in that sample. The latter value was calculated for each sample as the product of the percentage of $CD45^+$ cells and the original hemocytometer count of total cells identified within that sample.

Statistical analysis

All data are presented as mean ± SEM of four to five (Figs. 1–3) or four to nine (Figs. 4, 6–9, Supplemental Figs. 1, 2) mice per group. Multiple cohort data were analyzed by ANOVA with post hoc Fisher least significant difference test for multiple comparisons. Two cohort comparisons were performed by Student *t* test. A p value <0.05 was considered significant in all cases.

Results

Persistent cryptococcal lung infection is associated with increased PD-1 expression on polarized $CD4^+$ T cells

The first objective of this study was to determine whether the PD-1 signaling pathway is upregulated in response to cryptococcal lung infection. To establish persistent cryptococcal lung infection, we inoculated C57BL/6 mice with *C. neoformans* strain 52D via the intratracheal route. At 0, 2, 3, and 4 WPI, pulmonary fungal burden was quantified by CFU assays, and $CD45^+$ lung leukocytes were enumerated by flow cytometric analysis. Fungal burden increased to $\sim 10^6$–10^7 CFU by 2 WPI and then remained at the same level throughout the duration of the study (Fig. 1A), consistent with other studies performed using this model system (10, 17, 37–40). Persistent infection was associated with a sustained accumulation of lung leukocytes (Fig. 1B). Histologic evaluation of lung sections obtained from mice at 4 WPI (Fig. 1C, 1D) identified characteristic features of persistent infection including the presence of numerous cryptococci, many of them located intracellularly within large macrophages. Loose alveolar infiltrates containing extracellular crystals, eosinophils, and small mononuclear cells with lymphocyte morphology were readily observed.

We used flow cytometric analysis of lung leukocytes obtained at 2, 3, and 4 WPI to assess whether lymphocytes present in these immune infiltrates expressed PD-1 (Fig. 2A–I). Our results demonstrated that persistent cryptococcal lung infection is associated with a robust and sustained 2- to 3-fold increase in the total numbers of $CD4^+$ T cells in the lung at 2, 3, and 4 WPI. $CD8^+$ T cell numbers were increased only at 4 WPI, whereas the relatively small numbers of δγ T cells briefly increased at 2 and 3 WPI but returned to baseline thereafter. A nonsignificant trend toward increased accumulation of B cells was also observed. We found that PD-1 expression was significantly increased on $CD4^+$, $CD8^+$, and δγ T cells in the lungs of persistently infected mice as early as 2 WPI relative to expression on T cells in uninfected mice (Fig. 2J). PD-1 expression remained elevated on $CD4^+$ and $CD8^+$ T cells at 3 and 4 WPI, whereas expression of PD-1 on γδ T cells returned to baseline by 4 WPI.

To evaluate PD-1 expression on specific Th subsets, we used intracellular staining of the nuclear transcription factors T-bet, *Rorγt*, Gata3, and Foxp3 to identify Th1, Th17, Th2, and T regulatory (Treg) cells, respectively (refer to Fig. 2A–H). Using this approach, our data demonstrated that the numbers of Th1 and Th17 cells increased 2- to 3-fold relative to uninfected mice, whereas the number of Th2 cells and Treg cells increased 4- to 5-fold (Fig. 2K). In uninfected mice, PD-1 expression on each Th subset was <10% (Fig. 2L). In response to infection, PD-1 expression

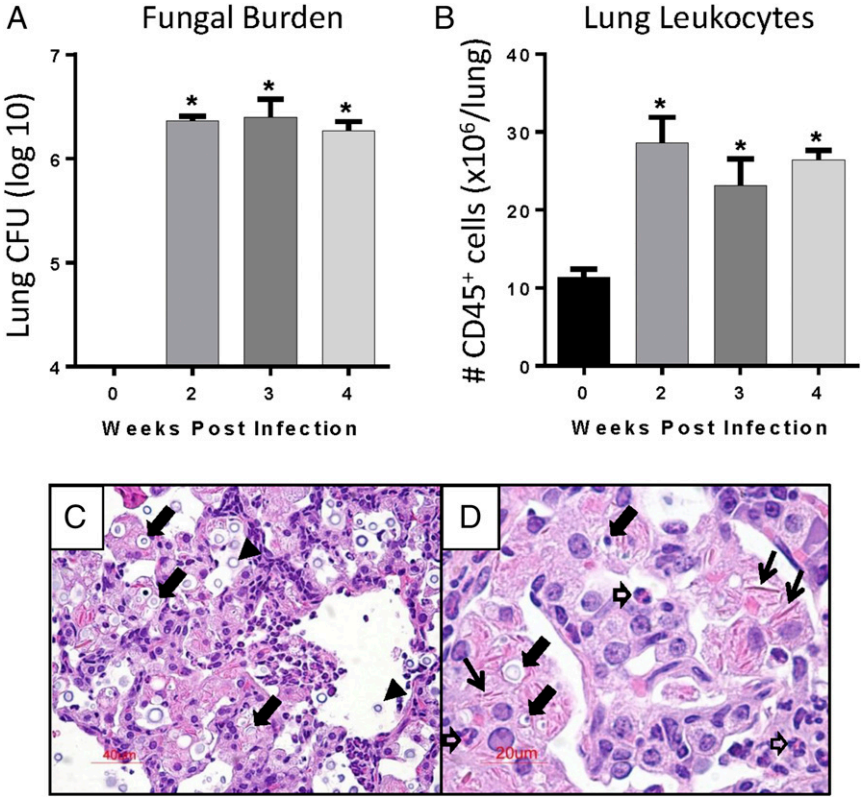

FIGURE 1. Induction of persistent cryptococcal lung infection in C57BL/6 mice. (**A**–**D**) C57BL/6 mice were infected by the intratracheal route with *C. neoformans* strain 52D. At day 0 (uninfected) and 2, 3, and 4 WPI, lungs were harvested for analysis. (A) Fungal lung burden was assessed using CFU assays. (B) Number of $CD45^+$ lung leukocytes was assessed using flow cytometric analysis. (C and D) Representative lung sections (H&E stain) from infected mice at 4 WPI. Original magnification ×200 (C), ×400 (D). Note the presence of numerous intracellular cryptococci within macrophages (solid block arrows), extracellular cryptococci in the alveolar space (arrowheads), eosinophils (open block arrows), and extracellular crystals (thin arrows). (A and B) n = 4–5 mice assayed individually per time point. $*p < 0.05$ by ANOVA with Fisher least significant difference post hoc test versus day 0 (uninfected).

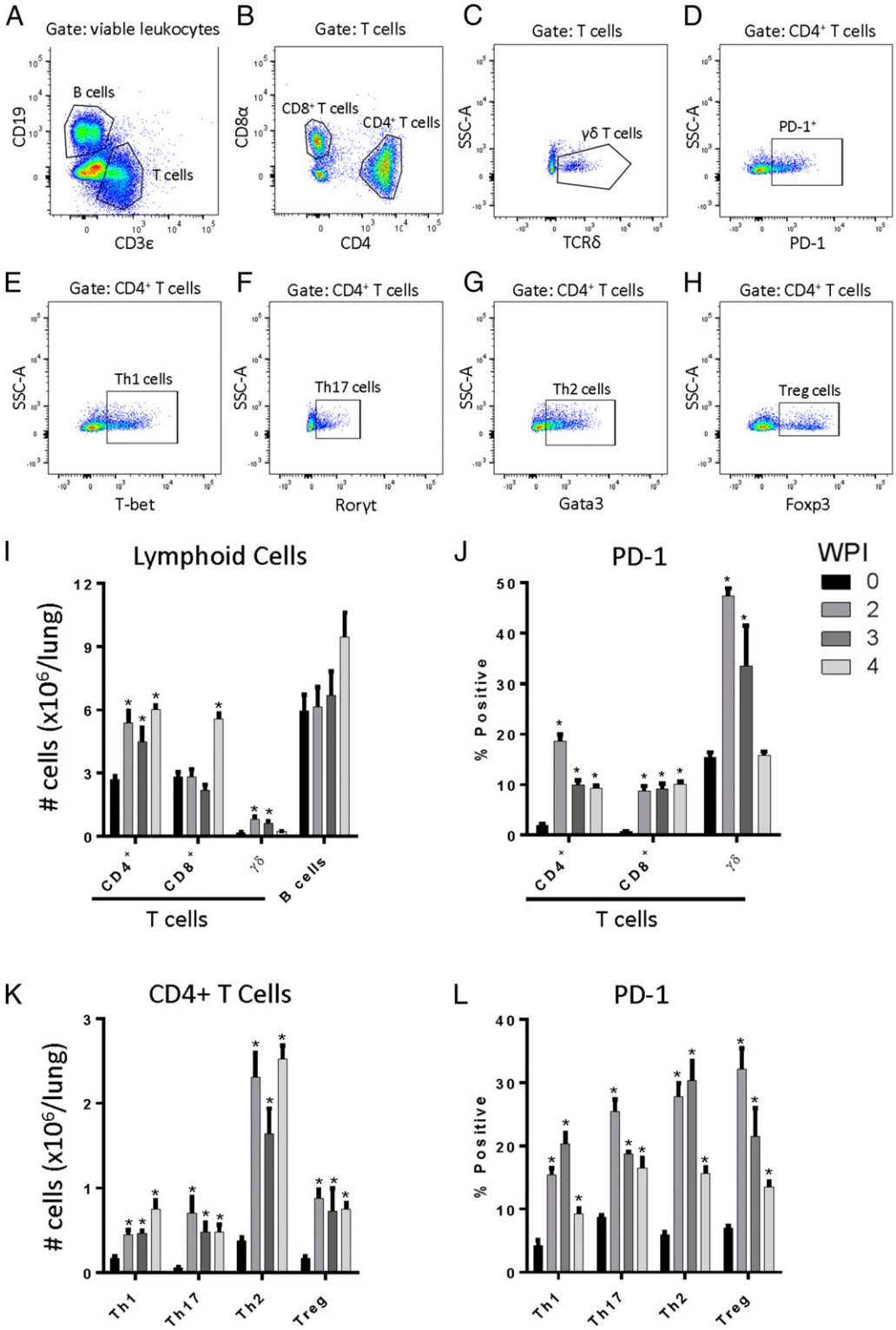

FIGURE 2. Persistent cryptococcal lung infection promotes lymphoid cell accumulation and increased T cell PD-1 expression. Following infection of mice with *C. neoformans* strain 52D, lungs were collected and processed for flow cytometry analysis at 0, 2, 3, and 4 WPI. Lung single-cell suspensions were subjected to 12-color flow cytometry for analysis of lymphoid cell populations and PD-1 expression (**A**–**H**). Representative gating on cells obtained at 3 WPI is shown. After selection of viable leukocytes based on expression of CD45 and a viability dye (data not shown), T and B cells were characterized based on expression of CD19 (B cells) (A) or CD3ε (T cells) (A). Next, subsets of T cells were characterized by expression of CD8α ($CD8^+$ T cells) (B), CD4 ($CD4^+$ T cells) (B), or TCRδ (γδ T cells) (C). Representative PD-1 staining pattern for $CD4^+$ T cells is shown (D). Subsets of $CD4^+$ T cells were characterized based on expression of hallmark transcription factors T-bet (Th1 cells) (E), *Rorγt* (Th17 cells) (F), Gata3 (Th2 cells) (G), and Foxp3 (Treg cells) (H). (**I**–**L**) Application of this gating scheme facilitated (I) the enumeration of specific lymphocyte subsets, (J) PD-1 expression on lymphocytes subsets, (K) enumeration of $CD4^+$ T cell subsets, and (L) PD-1 expression on $CD4^+$ T cell subsets. (I–L) $n = 4$–5 mice assayed individually per time point. $^*p < 0.05$ by ANOVA with Fisher least significant difference post hoc test versus day 0 (uninfected).

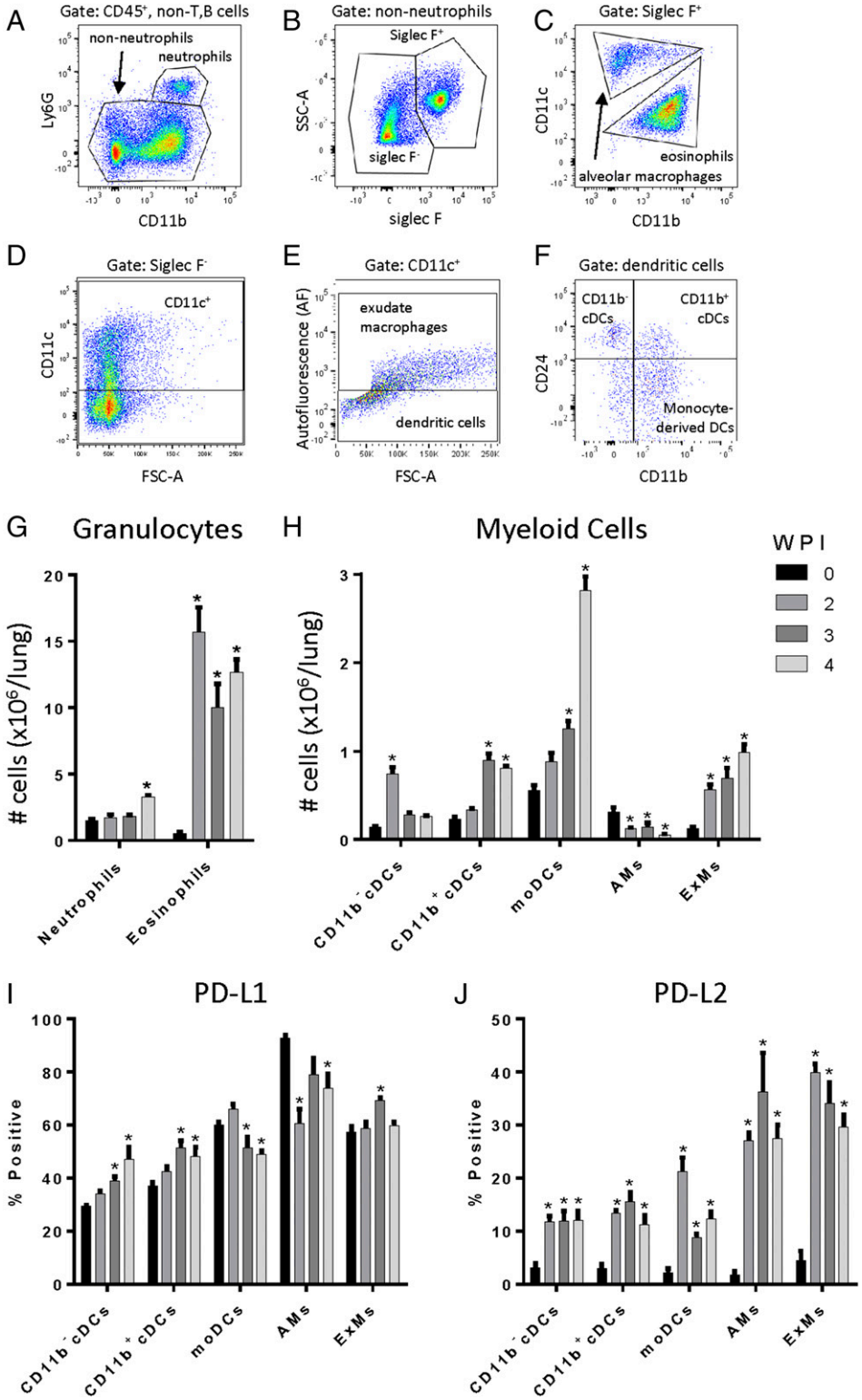

FIGURE 3. Persistent cryptococcal lung infection causes accumulation of numerous myeloid cell populations and increased DC and macrophage PD-L1 and PD-L2 expression. Single-cell suspensions of lung cells were subjected to 12-color flow cytometry for analysis of myeloid cell populations (**A**–**F**). Representative gating on cells obtained at 3 WPI is shown. After selection of viable leukocytes (data not shown), T and B cells were excluded by expression of CD19 or TCRβ (data not shown). Next, neutrophils were characterized based on expression of CD11b and Ly6G (A). Nonneutrophils were then separated into Siglec F^+ and Siglec F^- populations (B). Within the Siglec F^+ population, AMs were identified as $CD11b^-CD11c^+$, whereas eosinophils were defined as $CD11b^+CD11c^-$ (C). Siglec F^- cells were gated on $CD11c^+$ cells (D). The Siglec F^-CD11c^+ population was divided into ExMs and DCs; ExMs were characterized as autofluorescence (AF^+), whereas DCs were AF^- (E). DCs were divided into three subgroups based on expression of CD24 and CD11b (F): $CD11b^-$ cDCs ($CD24^+CD11b^-$; i.e., $CD103^+$ DCs), $CD11b^+$ cDCs ($CD24^+CD11b^+$), and moDCs ($CD24^-CD11b^+$). (**G** and **H**) Application of this gating scheme facilitated the enumeration of (G) granulocyte subsets and (H) myeloid cell subsets, including $CD11b^-$ and $CD11b^+$ cDCs, moDCs, AMs, and ExMs. Expression of PD-L1 and PD-L2 on myeloid cells was assessed by flow cytometry. Relative expression of PD-L1 (**I**) and PD-L2 (**J**) on DCs and macrophages is shown. (G–J) n = 4–5 mice assayed individually per time point. *$p < 0.05$ by ANOVA with Fisher least significant difference post hoc test versus day 0 (uninfected).

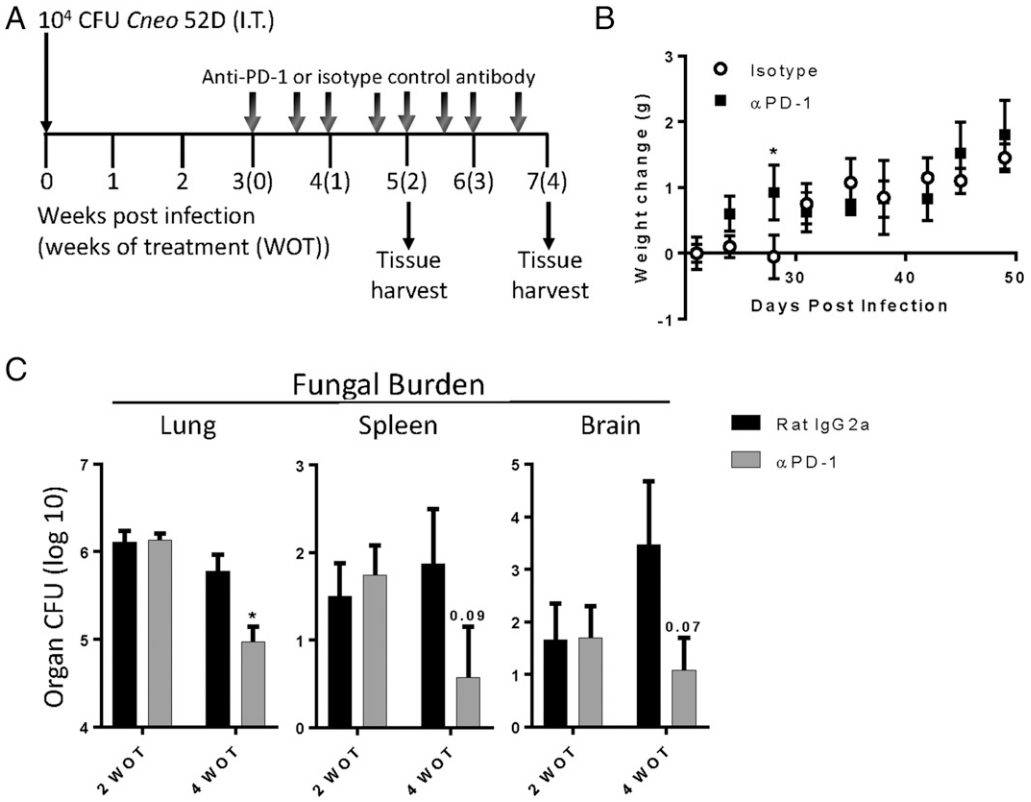

FIGURE 4. Anti–PD-1 Ab treatment promotes fungal clearance in mice with cryptococcal lung infection. (**A**) C57BL/6 mice were infected intratracheally with *C. neoformans* strain 52D. Beginning at 3 WPI, mice were administered 200 μg of either neutralizing anti–PD-1 Ab (RMP1-14) or isotype-matched control Ab (2A3) twice per wk for 2–4 wk of treatment (WOT). (**B**) Weight change in cohorts of treated mice. (**C**) Fungal burden in lungs, spleens, and brains of treated cohorts of mice. (B and C) n = 4–9 per cohort assayed individually in two separate experiments. *$p < 0.05$ by unpaired Student t test.

increased to between 20 and 30% on each Th subset and remained elevated relative to uninfected mice at all time points studied. Collectively, our findings demonstrate increased PD-1 expression on $CD4^+$, $CD8^+$, and γδ T cells accumulating in the lungs of mice that develop persistent cryptococcal infection. Moreover, increased PD-1 expression was not limited to any one subset of $CD4^+$ T cells; rather, PD-1 expression was comparably increased and sustained on Th1, Th17, Th2, and Treg cells (Fig. 2L), suggesting that the preferential enhancement of Th2 responses observed in this model is not attributable to differential expression of PD-1.

Persistent cryptococcal lung infection is associated with increased expression of PD-L1 and PD-L2 on specific subsets of lung DCs and macrophages

We evaluated whether increased PD-1 expression on T cell subsets in the lung was associated with a concomitant increase in the expression of PD-1 ligands, PD-L1 and PD-L2, on lung myeloid cells. Specific subsets of lung DCs and macrophages were identified within lung leukocyte populations obtained at 0, 2, 3, and 4 WPI using flow cytometric analysis and a detailed gating scheme (refer to Refs. 8, 41, and 42 and Fig. 3A–F). Results demonstrated a significant 2-fold increase in the number of lung neutrophils present at 4 WPI and a significant 10- to 15-fold increase in the number of eosinophils present at all time points postinfection (Fig. 3G). Among DC populations (Fig. 3H), $CD11b^-$ conventional DC (cDC) numbers were increased 4-fold at 2 WPI followed by a return to baseline by 3 WPI, whereas the number of $CD11b^+$ cDCs was unchanged at 2 WPI but was increased 3-fold at 3 and 4 WPI (Fig. 3H). In contrast, numbers of nonresident monocyte-derived DCs (moDCs) increased almost 6-fold by 4 WPI at which point they outnumbered $CD11b^-$ DCs and $CD11b^+$ DCs by a 2:1 ratio. Among macrophage populations, numbers of resident AMs decreased postinfection, whereas we observed a progressive 5-fold expansion in recruited exudate macrophages (ExMs) by 4 WPI (Fig. 3H). In response to infection, lung macrophages demonstrated increased intracellular staining for the M2 activation marker, arginase, but not the M1 activation marker, iNOS, consistent with an alternatively activated phenotype (data not shown).

In uninfected mice, PD-L1 was expressed on ∼30–60% of lung DCs and 60–90% of macrophages (Fig. 3I). In response to infection, PD-L1 expression was modestly increased on $CD11b^-$ cDCs, $CD11b^+$ cDCs, and ExMs, whereas expression decreased slightly on moDCs and AMs (Fig. 3I). In contrast, PD-L2 was expressed on <5% of all myeloid cells in uninfected lungs, but its expression was markedly increased and sustained on all myeloid cell populations examined at 2, 3, and 4 WPI (Fig. 3J); increased PD-L2 expression was most prominent on alveolar and ExMs, with 30–40% of these populations expressing PD-L2 in response to persistent infection. Thus, our data reveal increased and sustained lung myeloid cell expression of PD-L1 and PD-L2 in mice with persistent cryptococcal infection.

Anti–PD-1 Ab treatment improves fungal clearance in mice with persistent cryptococcal lung infection

Numerous studies have shown that blockade of the PD-1 signaling pathway can promote enhanced immune responses against cancers by altering important immunomodulatory mechanisms active in established tumor microenvironments (29–31, 43, 44). Having identified that PD-1 and its ligands were upregulated on immune effector cells in the lungs of mice with persistent cryptococcal lung infection, our next objective was to determine whether Ab-mediated blockade of this pathway could improve fungal clearance in this

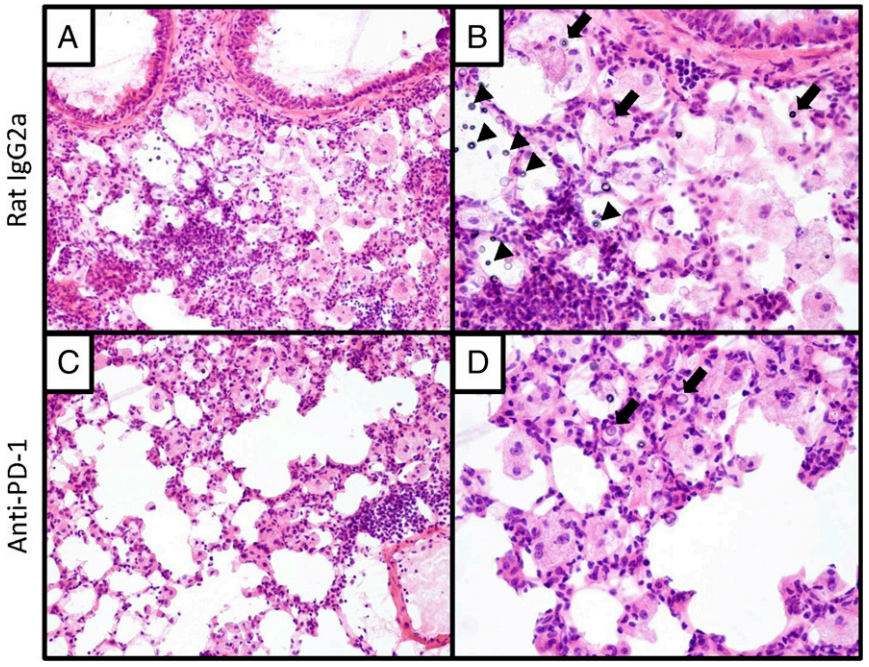

FIGURE 5. Effect of anti–PD-1 Ab treatment on lung histopathology. Representative lung sections obtained from mice treated (at 3 WPI) with control (**A** and **B**) and anti–PD-1 Ab (**C** and **D**) for 4 wk. Sections were H&E-stained and examined by light microscopy. Original magnification ×200 (A and C), ×400 (B and D). Sections at low magnification (A and C) show similar overall immune cell infiltration between treatments. Sections obtained from the isotype-treated group at high magnification (B) show numerous cryptococci located both intracellularly (arrows) and extracellularly (arrowheads). Sections obtained from the anti–PD-1–treated group at high magnification (D) reveal fewer cryptococci and a diminished number of foamy macrophages (relative to control-treated mice).

model. We administered neutralizing anti–PD-1 Ab or isotype control Ab twice per wk at a dose of 200 μg/mouse (see *Materials and Methods*; Fig. 4A). Treatment was initiated at 3 WPI and continued for 2 or 4 wk, at which times fungal burden in the lung, spleen, and brain was assessed. During the period of Ab administration, no significant weight loss (Fig. 4B) or alterations in animal behavior scores (data not shown) were observed between cohorts of mice treated with anti–PD-1 versus control Ab. Our results showed that 2 wk of treatment (WOT) with anti–PD-1 Ab did not significantly alter fungal burden in the lungs, brains, or

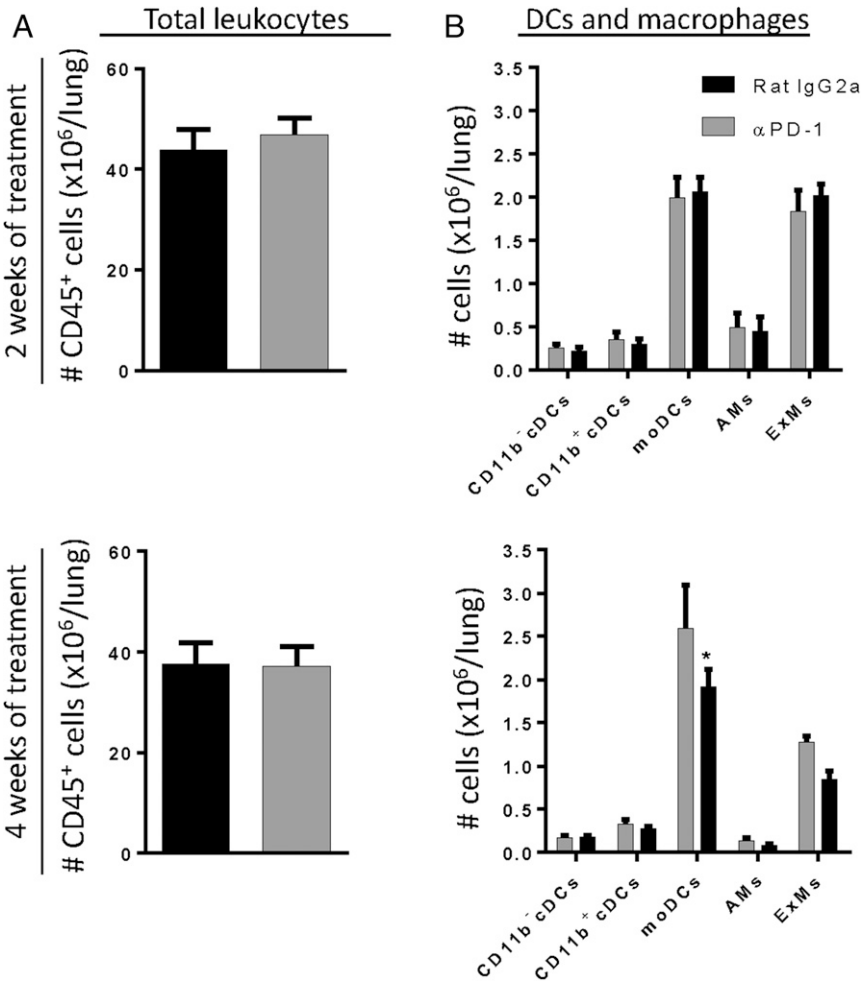

FIGURE 6. Anti–PD-1 Ab treatment does not substantially alter lung myeloid cell accumulation in the lungs of mice with cryptococcal lung infection. Infected C57BL/6 mice treated with either neutralizing anti–PD-1 Ab or control Ab were evaluated (by flow cytometric analysis) at 2 WOT (top panels) or 4 WOT (bottom panels) for numbers of (**A**) total lung $CD45^+$ leukocytes and (**B**) subsets of lung DCs and macrophages. $n = 4–9$ per cohort assayed individually in two separate experiments. $*p < 0.05$ by unpaired Student t test.

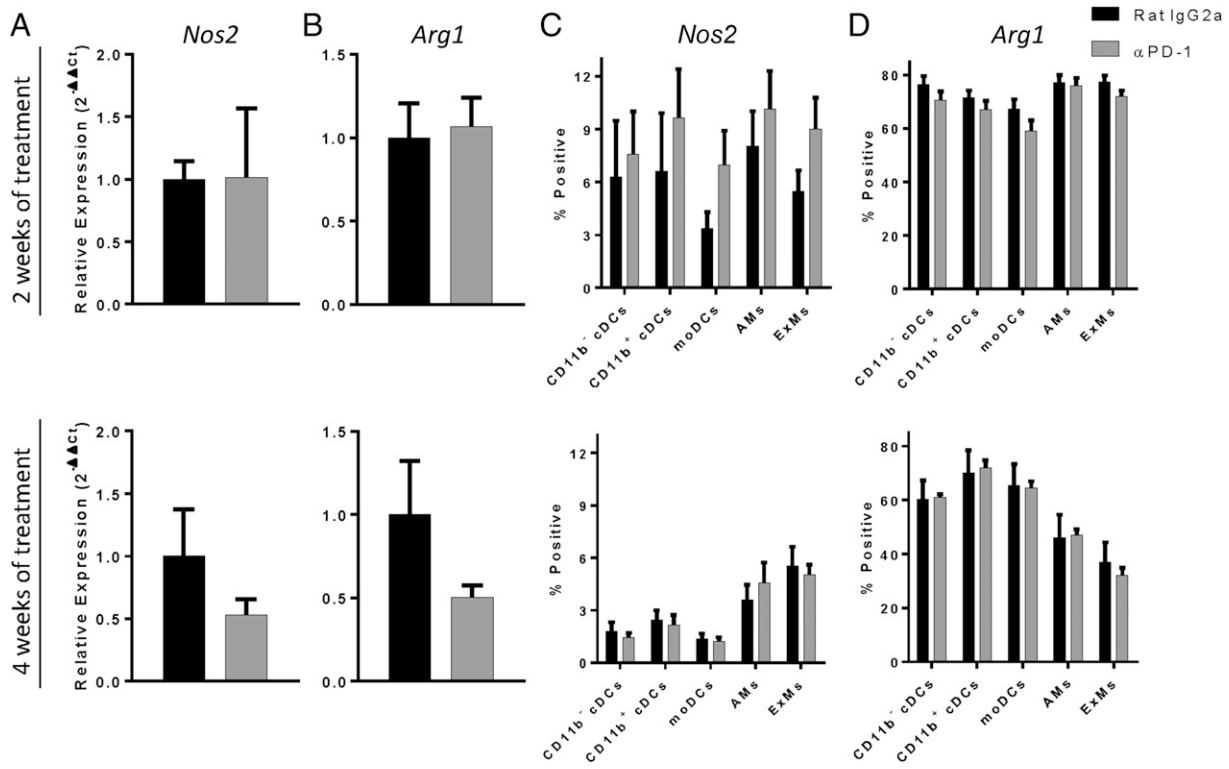

FIGURE 7. Anti–PD-1 Ab treatment does not substantially alter lung myeloid cell activation in the lungs of mice with cryptococcal lung infection. Infected C57BL/6 mice treated with either neutralizing anti–PD-1 or control Ab were evaluated for iNOS and arginase expression by (**A** and **B**) qPCR for *Nos2* and *Arg1* and (**C** and **D**) flow cytometric analysis for intracellular protein staining using lung leukocytes obtained at 2 WOT (top panels) or 4 WOT (bottom panels). For (A) and (B), $n = 4–9$ per cohort assayed individually in two separate experiments. $^*p < 0.05$ by unpaired Student t test.

spleens of infected mice relative to isotype control-treated mice (Fig. 4C). However, mice treated for 4 wk with anti–PD-1 Ab displayed significant reductions in pulmonary fungal burden relative to isotype control-treated mice (Fig. 4C); nonsignificant trends toward reduced fungal burden in the brains and spleens of anti–PD-1 Ab–treated mice were also observed.

We considered whether Ab administration might directly alter fungal growth. Data from our prior study investigating the effects of Ab-mediated IL-10 blockade demonstrated comparable pulmonary fungal burden at 5 WPI in mice receiving isotype control Ab relative to infected but untreated mice (17). In addition, data from this study show that mice treated with isotype control Ab remained persistently infected (pulmonary fungal burdens near 6 log CFUs; Fig. 4C). Furthermore, we observed no alteration in fungal growth in vitro when *C. neoformans* was cultured for 24 or 48 h in the presence of two different doses (0.8 or 8.0 μg/ml) of either isotype control (IgG2A) or anti–PD-1 Abs (relative to *C. neoformans* cultured with no Ab added; data not shown). These collective data suggest that the Abs administered to mice in this study did not directly alter fungal growth. Thus, given the additional animal use required and the logistical complexity involved, additional cohorts of infected but untreated mice were not included in our in vivo studies assessing the effects of Ab-mediated PD-1 blockade.

We assessed microanatomic features of PD-1 blockade by histologic evaluation using lung sections obtained from infected mice treated for 4 wk with either isotype control Ab or anti–PD-1 Ab (Fig. 5). In control mice, we observed numerous intracellular and extracellular cryptococci located in patchy alveolar infiltrates composed of numerous mononuclear cells, eosinophils, and larger cells with abundant cytoplasm consistent with macrophage morphology (Fig. 5A, 5B). In mice treated with anti–PD-1 Ab, the overall number of lung leukocytes appeared comparable with that observed in isotype control Ab-treated mice; however, the number of cryptococci identified, especially those located extracellularly, appeared markedly reduced, as did the number of foamy macrophages (Fig. 5C, 5D). Collectively, our data demonstrate that anti–PD-1 Ab treatment in mice with established cryptococcal lung infection promotes fungal clearance in the lung and may reduce systemic fungal dissemination.

Anti–PD-1 Ab treatment does not alter the accumulation or activation profile of lung myeloid cells in mice with persistent cryptococcal lung infection

Our next objective was to investigate cellular and molecular pathways altered by PD blockade. We first sought to determine whether differences in fungal burden between anti–PD-1 and control Ab-treated mice were associated with changes in the accumulation of myeloid cells in the lung. Our results show that anti–PD-1 Ab treatment did not alter the total number of accumulating lung leukocytes (Fig. 6A) or the number of any specific subset of accumulating DCs or macrophages (Fig. 6B) in the lung after 2 or 4 WOT (top and bottom panels, respectively) as compared with control-treated mice, with the exception of a small reduction in the number of moDCs after 4 WOT (Fig. 6B, bottom panel).

Because minimal differences in lung myeloid cell numbers were identified after treatment with anti–PD-1 Ab, we determined whether PD-1 blockade altered the activation profile of lung myeloid cells in treated mice. Our findings demonstrated that PD-1 blockade did not alter gene expression of either iNOS (*Nos2*) or arginase (*Arg1*) by total lung leukocytes (Fig. 7A, 7B) or intracellular staining for iNOS or arginase within any lung DC or macrophage subset studied after either 2 or 4 WOT (Fig. 7C, 7D). Treatment with anti–PD-1 Ab also did not affect DC or macrophage cell surface expression of two other molecules associated with classical activation, MHC

class II and CD80, after either 2 or 4 WOT (data not shown). Note that for all myeloid cell subsets, intracellular staining for arginase was considerably greater than that of iNOS, consistent with a predominantly alternatively activated (M2) phenotype. Taken together, these data demonstrate that changes in pulmonary fungal burden in anti–PD-1–treated mice are not associated with substantial differences in the accumulation or activation of lung DCs or macrophages.

Anti–PD-1 Ab treatment reduces IL-5 *and* IL-10 *gene expression by lung leukocytes in mice with persistent cryptococcal lung infection*

We next investigated whether anti–PD-1 Ab treatment altered gene expression of immunostimulatory cytokines (IFN-γ and IL-17a) and immunomodulatory cytokines (IL-5 and IL-10) known to influence fungal clearance (9, 11, 12, 14, 16, 17). Our data showed no significant difference in gene expression of IFN-γ (*Ifng*) or IL-17a (*Il17a*) by total lung leukocytes between treatment groups at either 2 or 4 WOT (Supplemental Fig. 1). In contrast, expression of IL-5 (*Il5*) was significantly reduced in leukocytes of anti–PD-1 versus control Ab-treated mice after 2 WOT and trended toward a reduction after 4 WOT (Fig. 8A). Gene expression of IL-10 (*Il10*) was significantly reduced after anti–PD-1 Ab treatment after 4 WOT (Fig. 8B). Thus, anti–PD-1 Ab treatment reduces gene expression of two cytokines associated with fungal persistence.

Anti–PD-1 treatment does not alter accumulation of polarized CD4$^+$ T cells in the lungs of mice with persistent cryptococcal lung infection but does enhance sustained expression of OX40 by Th1 and Th17 cells

Our final objective was to determine whether PD-1 blockade altered accumulation and activation of lymphoid cell subpopulations in the lungs of mice with persistent cryptococcal lung infection. We observed that treatment with anti–PD-1 Ab did not alter the number of B cells, total T cells, CD8$^+$ T cells, or γδ T cells relative to control mice (Supplemental Fig. 2). Moreover, PD-1 blockade did not significantly affect accumulation of any specific subset of polarized CD4$^+$ Th cells, including Th1, Th17, Th2, or Treg cells, at either of the two time points studied (Fig. 9A).

Because PD-1 blockade did not change the number of T cells or CD4$^+$ Th subsets, we investigated whether treatment with anti–PD-1 Ab altered T cell activation status. We examined the expression of ICOS, known to be important in secondary stimulation of activated T cells (45), and OX40, which promotes memory T cell responses and has previously been shown to enhance fungal clearance in *C. neoformans*–infected mice when treated with a receptor agonist (46). Our data showed that 2 WOT with anti–PD-1 Ab significantly increased the expression of both ICOS and OX40 on all subsets of CD4$^+$ T cells (except for ICOS expression on Th17 cells; Fig. 9B, 9C, top panels). After 4 WOT, ICOS expression had decreased back to baseline, whereas OX40 expression remained upregulated on Th1 and Th17 cells, but not on Th2 or Treg cells (Fig. 9C, bottom panels). These collective results suggest that improved fungal clearance in response to targeted PD-1 signaling blockade in mice with persistent cryptococcal lung infection is mediated, at least in part, through beneficial effects on CD4$^+$ T cell activation, including the sustained upregulation of OX40 on Th1 and Th17 cells.

Discussion

PD-1 signaling has proven beneficial by modulating immune effector responses and preventing autoimmunity. In contrast, our findings contribute to an emerging body of evidence demonstrating that PD-1 signaling can contribute to immune evasion by tumors and certain invading pathogens. Using a murine model of persistent cryptococcal lung infection, our study provides the following novel observations: 1) PD-1 expression is both increased and sustained on broad subsets of T cells in the lungs; 2) expression of the PD-1 ligands, PD-L1 and PD-L2, is enhanced on specific subsets of lung DCs and macrophages; and 3) targeted PD-1 blockade improves fungal clearance. Our additional studies suggest that the beneficial effects of anti–PD-1 Ab treatment may be mediated through reductions of detrimental IL-5 and IL-10 cytokines, and increased activation of Th1 and Th17 cells. Collectively, these data provide

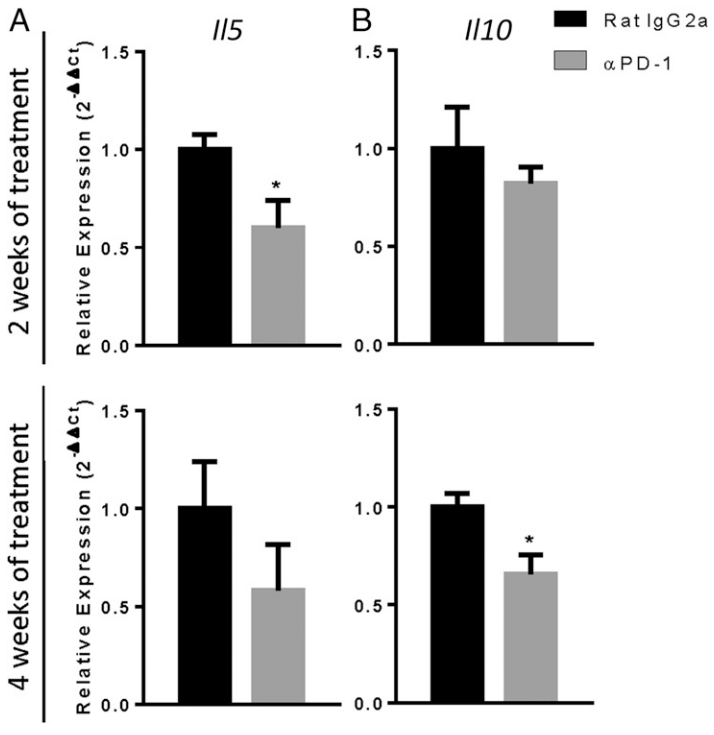

FIGURE 8. Anti–PD-1 Ab treatment decreases IL-5 and IL-10 gene expression in mice with cryptococcal lung infection. Infected C57BL/6 mice treated with either neutralizing anti–PD-1 or control Ab were evaluated for gene expression by qRT-PCR for (**A**) IL-5 (*Il5*) and (**B**) IL-10 (*Il10*) using lung leukocytes obtained at 2 (top panels) or 4 WOT (bottom panels). n = 4–9 per cohort assayed individually in two separate experiments. *$p < 0.05$ by unpaired Student t test.

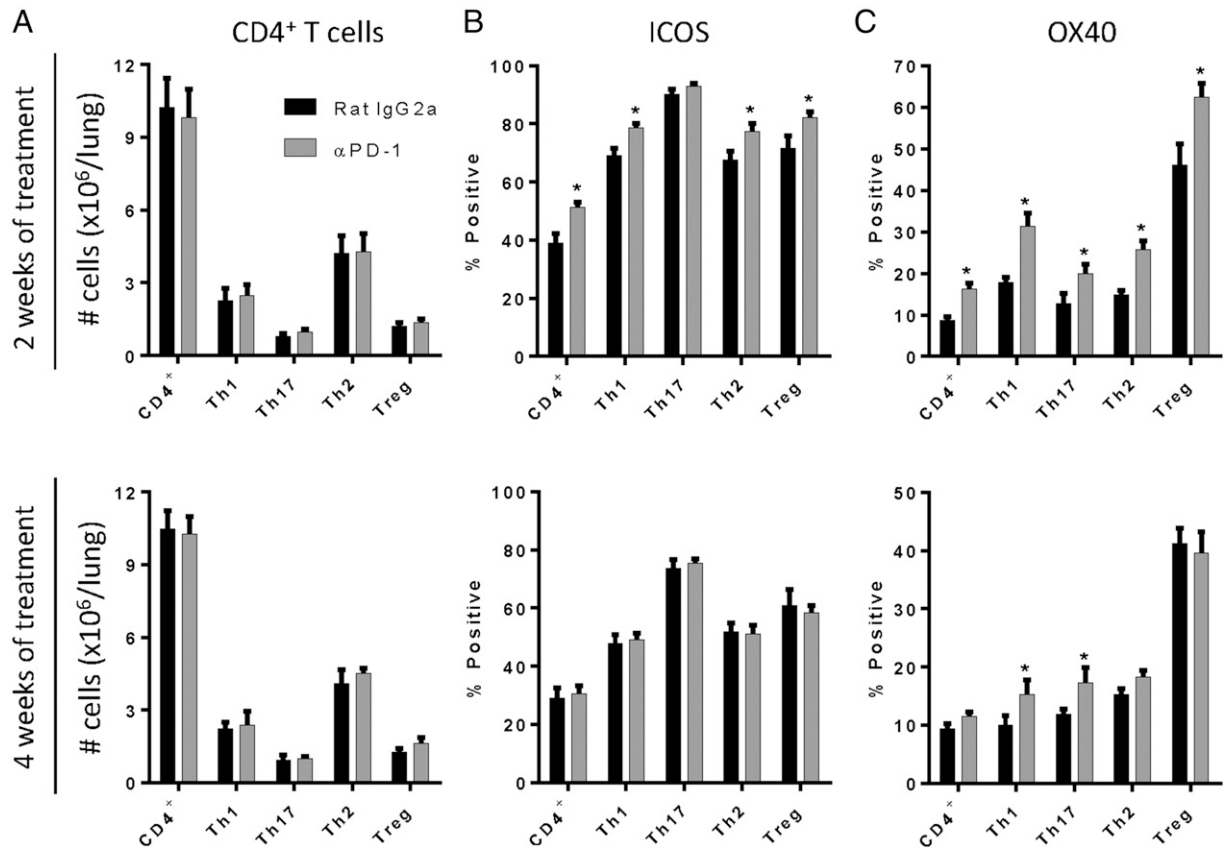

FIGURE 9. Anti–PD-1 Ab treatment promotes sustained expression of ICOS and OX40 on Th1 and Th17 cells. Infected C57BL/6 mice treated with either neutralizing anti–PD-1 or control Ab were evaluated (by flow cytometric analysis) at 2 (top panels) or 4 WOT (bottom panels) for (**A**) total numbers of $CD4^+$ T cells and $CD4^+$ T cell subsets and their expression of T cell activation markers including (**B**) ICOS and (**C**) OX40. (A–C) $n = 4–9$ per cohort assayed individually in two separate experiments. $*p < 0.05$ by unpaired Student t test.

strong evidence that the PD-1 signaling pathway promotes persistence of cryptococcal lung infection and opens new avenues for the development of novel immune-based treatments for the treatment of chronic fungal diseases.

Our thorough kinetic evaluation of the expression of PD-1 and its ligands (PD-L1 and PD-L2) demonstrates that persistent cryptococcal lung infection is associated with sustained expression of this immunomodulatory pathway. The data show that PD-1 expression was increased on multiple lymphocyte subsets including all four major subsets of polarized $CD4^+$ Th cells residing in the lungs of infected mice. This finding argues that the relative skewing of the adaptive immune response toward a nonprotective Th2/Treg bias in this model is not attributable to selectively limited or enhanced expression of PD-1 on any one (or more) Th subset. We similarly identified broad and sustained expression of PD-L1 and PD-L2 by numerous subsets of lung DCs and macrophages, although the expression tended to be highest on lung macrophages. These observations confirm and extend those of Guerrero et al. (33), who demonstrated increased expression of PD-L1 and PD-L2 on AMs in the lungs of C57BL/6 mice infected with *C. neoformans* strain 52D. Interestingly, although that study only assessed PD-L1 and PD-L2 expression on AMs, it showed that increased expression of both ligands was associated with a more virulent, mucoid strain of the organism, providing further evidence that fungal virulence factors may exploit this pathway to promote immune evasion. Our results also show that of the two ligands, PD-L2 is more dynamically responsive to changes in the infected lung microenvironment, whereas the degree of PD-L1 upregulation is less prominent. This finding may be explained by the prominence of Th2 responses observed in this model because Loke and Allison (47) have previously shown that PD-L1 is widely expressed by peritoneal macrophages at baseline with increased expression in response to LPS, IFN-γ, and IL-4, whereas PD-L2 expression is initially more restricted and is more specifically increased in response to a key T2 cytokine, IL-4.

Our observation that treatment of persistently infected mice for 4 wk with anti–PD-1 blocking Ab significantly improved fungal clearance within the lung provides direct evidence that the PD-1 signaling pathway actively opposes fungal clearance. The effect was not immediate, as 2 WOT did not improve fungal clearance, although treatment may have begun to enhance specific immune effector mechanisms at this time point (see later). Our decision to treat with anti–PD-1 Ab was informed by our observation that both PD-L1 and PD-L2 are prominently expressed once persistent infection is established; thus, we sought to effectively block input from both of these ligands. In addition to significantly reducing the fungal burden in the lung, treatment was also associated with a trend toward reductions in fungal burden in the spleen and brain, suggesting that enhanced fungal containment in the lung reduced systemic dissemination of the organism. Alternatively, it is possible that PD-1 blockade enhanced immunity in secondary infection sites including the CNS. The presence of organisms in the lung and brain shows that the current treatment protocol did not achieve sterilizing immunity, and we suspect some mice in the anti–PD-1 Ab–treated group might eventually die, perhaps of meningitis. Future studies are warranted to investigate whether reduced dissemination and/or enhanced immunity are the cause of reduced fungal burdens in the spleens and brains of anti–PD-1–treated mice.

The improvement in fungal clearance we observe in mice with established cryptococcal lung infection treated with anti–PD-1 Ab support and extend the findings of two prior studies showing that PD-1 deficiency or blockade improved fungal clearance and/or survival of infection with *Histoplasma capsulatum* or *Candida albicans* (35, 36). In both of these studies, the investigators assessed the effects of PD-1 blockade throughout the entire duration of the infections, which were both acute and lethal. In this study, we show that treatment with anti–PD-1 Ab is effective, even when PD-1 blockade is delayed until after persistent infection has been established. Thus, the results of our study suggest that PD-1 blockade might be effective at treating patients already infected with a fungal pathogen.

Anti–PD-1 Ab treatment did not result in substantial weight loss, abnormal animal behavior, or increase the total number of lung leukocytes (or any leukocyte subset). Thus, there was no evidence that PD-1 blockade in mice with fungal infection caused pneumonitis or any other form of immune reconstitution syndrome (48, 49) in a manner detrimental to the mice. Although we had correctly hypothesized that treatment would improve fungal clearance, it was possible that treatment might have enhanced susceptibility to infection; this did not occur, however. Given the widespread use of checkpoint inhibitors in patients with cancer, these data provide a measure of reassurance that the inadvertent treatment of patients with unrecognized underlying fungal infection is unlikely to cause harm.

Our data provide several key insights into the cellular and molecular mechanisms that might explain the improved fungal clearance observed in response to anti–PD-1 Ab treatment. Notably, PD-1 blockade had a minimal effect on the number of immune effector cells in the lung. This finding differed from our study performed using an anti–IL-10R blocking Ab in which we attributed improved fungal clearance to its ability to increase the number of several effector cells including moDCs, ExMs, and Th1 and Th17 cells (17). However, our findings do suggest some interrelationship between the PD-1 and IL-10 immunomodulatory pathways because we found evidence that anti–PD-1 Ab treatment diminished IL-10 gene expression. IL-5 gene expression was also reduced by PD-1 blockade. Because both IL-10 and IL-5 are associated with nonprotective Th2 responses (9, 11), it is likely that some of the beneficial effects of anti–PD-1 Ab treatment were mediated through reductions in unfavorable T2 cytokine responses. As we have previously shown that inhibiting IL-10 signaling promotes fungal clearance (17), combined intervention toward both PD-1 and cytokine signaling pathways provides an intriguing avenue of possible future studies.

Treatment with anti–PD-1 Ab enhanced T cell expression of ICOS and OX40. Specifically, our findings demonstrate that 2 wk of anti–PD-1 treatment increased expression of ICOS on Th1, Th2, and Treg cells, but these effects were transient and not observed after 4 WOT. In contrast, whereas OX40 expression was increased on all polarized $CD4^+$ T cell populations after 2 wk of anti–PD-1 treatment, its expression remained elevated on Th1 and Th17 cells, but not on Th2 and Treg cells. Both molecules are associated with T cell activation (50, 51), and OX40 promotes memory T cell formation; thus, sustained activation of Th1 and Th17 cells as observed after 4 WOT may contribute to the beneficial effects of PD-1 blockade observed in this study. Support for this hypothesis is provided by a study by Humphreys et al. (46), which showed that engagement of OX40, utilizing an OX40L fusion protein, reduced pulmonary eosinophilia and promoted fungal clearance when evaluated in the identical model of murine cryptococcal lung infection used in this study. Thus, it might prove particularly informative to perform future studies seeking to determine whether combination therapy with PD-1 blockade and agonistic OX40L stimulation might further enhance clearance relative to either intervention alone. It would be of additional interest to determine whether the PD-1–expressing T cells are Ag specific and to assess whether the upregulation in OX40L in response to PD-1 blockade is limited to this T cell subset.

In summary, this study advances our understanding of molecular mechanisms that actively contribute to pathogen immune evasion and promote persistent infection. We specifically show that the PD-1 signaling pathway critically contributes to the pathogenesis of cryptococcosis, and our findings provide important proof of concept that checkpoint inhibitors may be incorporated into highly novel, immune-based therapies for the treatment of chronic fungal lung infections. These results motivate future studies seeking to further refine the appropriate dose and duration of therapy, and to assess the exciting possibility that anti–PD-1 Ab treatment in combination with conventional antibiotics or IL-10 signaling blockade might yield additive or synergistic results.

Acknowledgments

We acknowledge the enthusiastic input of Morgan Gordon, who provided additional scientific support of this project.

Disclosures

The authors have no financial conflicts of interest.

References

1. Li, S. S., and C. H. Mody. 2010. Cryptococcus. *Proc. Am. Thorac. Soc.* 7: 186–196.
2. Rajasingham, R., R. M. Smith, B. J. Park, J. N. Jarvis, N. P. Govender, T. M. Chiller, D. W. Denning, A. Loyse, and D. R. Boulware. 2017. Global burden of disease of HIV-associated cryptococcal meningitis: an updated analysis. *Lancet Infect. Dis.* 17: 873–881.
3. Bozzette, S. A., R. A. Larsen, J. Chiu, M. A. Leal, J. Jacobsen, P. Rothman, P. Robinson, G. Gilbert, J. A. McCutchan, J. Tilles, et al; California Collaborative Treatment Group. 1991. A placebo-controlled trial of maintenance therapy with fluconazole after treatment of cryptococcal meningitis in the acquired immunodeficiency syndrome. *N. Engl. J. Med.* 324: 580–584.
4. Chen, S., T. Sorrell, G. Nimmo, B. Speed, B. Currie, D. Ellis, D. Marriott, T. Pfeiffer, D. Parr, and K. Byth, Australasian Cryptococcal Study Group. 2000. Epidemiology and host- and variety-dependent characteristics of infection due to *Cryptococcus neoformans* in Australia and New Zealand. *Clin. Infect. Dis.* 31: 499–508.
5. Choi, Y. H., P. Ngamskulrungroj, A. Varma, E. Sionov, S. M. Hwang, F. Carriconde, W. Meyer, A. P. Litvintseva, W. G. Lee, J. H. Shin, et al. 2010. Prevalence of the VNIc genotype of *Cryptococcus neoformans* in non-HIV-associated cryptococcosis in the Republic of Korea. *FEMS Yeast Res.* 10: 769–778.
6. Mitchell, T. G., and J. R. Perfect. 1995. Cryptococcosis in the era of AIDS–100 years after the discovery of *Cryptococcus neoformans. Clin. Microbiol. Rev.* 8: 515–548.
7. Hsu, L. Y., E. S. Ng, and L. P. Koh. 2010. Common and emerging fungal pulmonary infections. *Infect. Dis. Clin. North Am.* 24: 557–577.
8. Chen, G. H., S. Teitz-Tennenbaum, L. M. Neal, B. J. Murdock, A. N. Malachowski, A. J. Dils, M. A. Olszewski, and J. J. Osterholzer. 2016. Local GM-CSF-dependent differentiation and activation of pulmonary dendritic cells and macrophages protect against progressive Cryptococcal lung infection in mice. *J. Immunol.* 196: 1810–1821.
9. Hernandez, Y., S. Arora, J. R. Erb-Downward, R. A. McDonald, G. B. Toews, and G. B. Huffnagle. 2005. Distinct roles for IL-4 and IL-10 in regulating T2 immunity during allergic bronchopulmonary mycosis. *J. Immunol.* 174: 1027–1036.
10. Hoag, K. A., N. E. Street, G. B. Huffnagle, and M. F. Lipscomb. 1995. Early cytokine production in pulmonary *Cryptococcus neoformans* infections distinguishes susceptible and resistant mice. *Am. J. Respir. Cell Mol. Biol.* 13: 487–495.
11. Huffnagle, G. B., M. B. Boyd, N. E. Street, and M. F. Lipscomb. 1998. IL-5 is required for eosinophil recruitment, crystal deposition, and mononuclear cell recruitment during a pulmonary *Cryptococcus neoformans* infection in genetically susceptible mice (C57BL/6). *J. Immunol.* 160: 2393–2400.
12. Jain, A. V., Y. Zhang, W. B. Fields, D. A. McNamara, M. Y. Choe, G. H. Chen, J. Erb-Downward, J. J. Osterholzer, G. B. Toews, G. B. Huffnagle, and M. A. Olszewski. 2009. Th2 but not Th1 immune bias results in altered lung functions in a murine model of pulmonary *Cryptococcus neoformans* infection. *Infect. Immun.* 77: 5389–5399.
13. Chen, G. H., R. A. McDonald, J. C. Wells, G. B. Huffnagle, N. W. Lukacs, and G. B. Toews. 2005. The gamma interferon receptor is required for the protective

pulmonary inflammatory response to *Cryptococcus neoformans*. *Infect. Immun.* 73: 1788–1796.
14. Arora, S., Y. Hernandez, J. R. Erb-Downward, R. A. McDonald, G. B. Toews, and G. B. Huffnagle. 2005. Role of IFN-gamma in regulating T2 immunity and the development of alternatively activated macrophages during allergic bronchopulmonary mycosis. *J. Immunol.* 174: 6346–6356.
15. Arora, S., M. A. Olszewski, T. M. Tsang, R. A. McDonald, G. B. Toews, and G. B. Huffnagle. 2011. Effect of cytokine interplay on macrophage polarization during chronic pulmonary infection with *Cryptococcus neoformans*. *Infect. Immun.* 79: 1915–1926.
16. Murdock, B. J., G. B. Huffnagle, M. A. Olszewski, and J. J. Osterholzer. 2014. Interleukin-17A enhances host defense against cryptococcal lung infection through effects mediated by leukocyte recruitment, activation, and gamma interferon production. *Infect. Immun.* 82: 937–948.
17. Murdock, B. J., S. Teitz-Tennenbaum, G. H. Chen, A. J. Dils, A. N. Malachowski, J. L. Curtis, M. A. Olszewski, and J. J. Osterholzer. 2014. Early or late IL-10 blockade enhances Th1 and Th17 effector responses and promotes fungal clearance in mice with cryptococcal lung infection. *J. Immunol.* 193: 4107–4116.
18. Osterholzer, J. J., R. Surana, J. E. Milam, G. T. Montano, G. H. Chen, J. Sonstein, J. L. Curtis, G. B. Huffnagle, G. B. Toews, and M. A. Olszewski. 2009. Cryptococcal urease promotes the accumulation of immature dendritic cells and a non-protective T2 immune response within the lung. *Am. J. Pathol.* 174: 932–943.
19. Olszewski, M. A., Y. Zhang, and G. B. Huffnagle. 2010. Mechanisms of cryptococcal virulence and persistence. *Future Microbiol.* 5: 1269–1288.
20. Qiu, Y., M. J. Davis, J. K. Dayrit, Z. Hadd, D. L. Meister, J. J. Osterholzer, P. R. Williamson, and M. A. Olszewski. 2012. Immune modulation mediated by cryptococcal laccase promotes pulmonary growth and brain dissemination of virulent *Cryptococcus neoformans* in mice. *PLoS One* 7: e47853.
21. Francisco, L. M., P. T. Sage, and A. H. Sharpe. 2010. The PD-1 pathway in tolerance and autoimmunity. *Immunol. Rev.* 236: 219–242.
22. Yamazaki, T., H. Akiba, H. Iwai, H. Matsuda, M. Aoki, Y. Tanno, T. Shin, H. Tsuchiya, D. M. Pardoll, K. Okumura, et al. 2002. Expression of programmed death 1 ligands by murine T cells and APC. *J. Immunol.* 169: 5538–5545.
23. Ishida, Y., Y. Agata, K. Shibahara, and T. Honjo. 1992. Induced expression of PD-1, a novel member of the immunoglobulin gene superfamily, upon programmed cell death. *EMBO J.* 11: 3887–3895.
24. Kaufmann, D. E., and B. D. Walker. 2009. PD-1 and CTLA-4 inhibitory cosignaling pathways in HIV infection and the potential for therapeutic intervention. *J. Immunol.* 182: 5891–5897.
25. Eichbaum, Q. 2011. PD-1 signaling in HIV and chronic viral infection–potential for therapeutic intervention? *Curr. Med. Chem.* 18: 3971–3980.
26. Barber, D. L., E. J. Wherry, D. Masopust, B. Zhu, J. P. Allison, A. H. Sharpe, G. J. Freeman, and R. Ahmed. 2006. Restoring function in exhausted CD8 T cells during chronic viral infection. *Nature* 439: 682–687.
27. Barber, D. L., K. D. Mayer-Barber, C. G. Feng, A. H. Sharpe, and A. Sher. 2011. CD4 T cells promote rather than control tuberculosis in the absence of PD-1-mediated inhibition. *J. Immunol.* 186: 1598–1607.
28. Rowe, J. H., T. M. Johanns, J. M. Ertelt, and S. S. Way. 2008. PDL-1 blockade impedes T cell expansion and protective immunity primed by attenuated *Listeria monocytogenes*. *J. Immunol.* 180: 7553–7557.
29. Iwai, Y., S. Terawaki, and T. Honjo. 2005. PD-1 blockade inhibits hematogenous spread of poorly immunogenic tumor cells by enhanced recruitment of effector T cells. *Int. Immunol.* 17: 133–144.
30. Hirano, F., K. Kaneko, H. Tamura, H. Dong, S. Wang, M. Ichikawa, C. Rietz, D. B. Flies, J. S. Lau, G. Zhu, et al. 2005. Blockade of B7-H1 and PD-1 by monoclonal antibodies potentiates cancer therapeutic immunity. *Cancer Res.* 65: 1089–1096.
31. Janakiram, M., V. Pareek, H. Cheng, D. M. Narasimhulu, and X. Zang. 2016. Immune checkpoint blockade in human cancer therapy: lung cancer and hematologic malignancies. *Immunotherapy* 8: 809–819.
32. Shrimali, R. K., J. E. Janik, R. Abu-Eid, M. Mkrtichyan, and S. N. Khleif. 2015. Programmed death-1 & its ligands: promising targets for cancer immunotherapy. *Immunotherapy* 7: 777–792.
33. Guerrero, A., N. Jain, X. Wang, and B. C. Fries. 2010. *Cryptococcus neoformans* variants generated by phenotypic switching differ in virulence through effects on macrophage activation. *Infect. Immun.* 78: 1049–1057.
34. Osterholzer, J. J., J. L. Curtis, T. Polak, T. Ames, G. H. Chen, R. McDonald, G. B. Huffnagle, and G. B. Toews. 2008. CCR2 mediates conventional dendritic cell recruitment and the formation of bronchovascular mononuclear cell infiltrates in the lungs of mice infected with *Cryptococcus neoformans*. *J. Immunol.* 181: 610–620.
35. Lázár-Molnár, E., A. Gácser, G. J. Freeman, S. C. Almo, S. G. Nathenson, and J. D. Nosanchuk. 2008. The PD-1/PD-L costimulatory pathway critically affects host resistance to the pathogenic fungus Histoplasma capsulatum. *Proc. Natl. Acad. Sci. USA* 105: 2658–2663.
36. Chang, K. C., C. A. Burnham, S. M. Compton, D. P. Rasche, R. J. Mazuski, J. S. McDonough, J. Unsinger, A. J. Korman, J. M. Green, and R. S. Hotchkiss. 2013. Blockade of the negative co-stimulatory molecules PD-1 and CTLA-4 improves survival in primary and secondary fungal sepsis. *Crit. Care* 17: R85.
37. Chen, G. H., D. A. McNamara, Y. Hernandez, G. B. Huffnagle, G. B. Toews, and M. A. Olszewski. 2008. Inheritance of immune polarization patterns is linked to resistance versus susceptibility to *Cryptococcus neoformans* in a mouse model. *Infect. Immun.* 76: 2379–2391.
38. Chen, G. H., M. A. Olszewski, R. A. McDonald, J. C. Wells, R. Paine, III, G. B. Huffnagle, and G. B. Toews. 2007. Role of granulocyte macrophage colony-stimulating factor in host defense against pulmonary *Cryptococcus neoformans* infection during murine allergic bronchopulmonary mycosis. *Am. J. Pathol.* 170: 1028–1040.
39. Arora, S., R. A. McDonald, G. B. Toews, and G. B. Huffnagle. 2006. Effect of a CD4-depleting antibody on the development of *Cryptococcus neoformans*-induced allergic bronchopulmonary mycosis in mice. *Infect. Immun.* 74: 4339–4348.
40. Huffnagle, G. B., G. B. Toews, M. D. Burdick, M. B. Boyd, K. S. McAllister, R. A. McDonald, S. L. Kunkel, and R. M. Strieter. 1996. Afferent phase production of TNF-alpha is required for the development of protective T cell immunity to *Cryptococcus neoformans*. *J. Immunol.* 157: 4529–4536.
41. Osterholzer, J. J., G. H. Chen, M. A. Olszewski, J. L. Curtis, G. B. Huffnagle, and G. B. Toews. 2009. Accumulation of CD11b+ lung dendritic cells in response to fungal infection results from the CCR2-mediated recruitment and differentiation of Ly-6Chigh monocytes. *J. Immunol.* 183: 8044–8053.
42. Misharin, A. V., L. Morales-Nebreda, G. M. Mutlu, G. R. Budinger, and H. Perlman. 2013. Flow cytometric analysis of macrophages and dendritic cell subsets in the mouse lung. *Am. J. Respir. Cell Mol. Biol.* 49: 503–510.
43. Okudaira, K., R. Hokari, Y. Tsuzuki, Y. Okada, S. Komoto, C. Watanabe, C. Kurihara, A. Kawaguchi, S. Nagao, M. Azuma, et al. 2009. Blockade of B7-H1 or B7-DC induces an anti-tumor effect in a mouse pancreatic cancer model. *Int. J. Oncol.* 35: 741–749.
44. Harvey, R. D. 2014. Immunologic and clinical effects of targeting PD-1 in lung cancer. *Clin. Pharmacol. Ther.* 96: 214–223.
45. Rudd, C. E., and H. Schneider. 2003. Unifying concepts in CD28, ICOS and CTLA4 co-receptor signalling. *Nat. Rev. Immunol.* 3: 544–556.
46. Humphreys, I. R., L. Edwards, G. Walzl, A. J. Rae, G. Dougan, S. Hill, and T. Hussell. 2003. OX40 ligation on activated T cells enhances the control of *Cryptococcus neoformans* and reduces pulmonary eosinophilia. *J. Immunol.* 170: 6125–6132.
47. Loke, P., and J. P. Allison. 2003. PD-L1 and PD-L2 are differentially regulated by Th1 and Th2 cells. *Proc. Natl. Acad. Sci. USA* 100: 5336–5341.
48. Gundacker, N. D., S. J. Jordan, B. A. Jones, J. C. Drwiega, and P. G. Pappas. 2016. Acute Cryptococcal immune reconstitution inflammatory syndrome in a patient on natalizumab. *Open Forum Infect. Dis.* 3: ofw038.
49. Hashimoto, H., S. Hatakeyama, and H. Yotsuyanagi. 2015. Development of cryptococcal immune reconstitution inflammatory syndrome 41 months after the initiation of antiretroviral therapy in an AIDS patient. *AIDS Res. Ther.* 12: 33.
50. Prell, R. A., D. E. Evans, C. Thalhofer, T. Shi, C. Funatake, and A. D. Weinberg. 2003. OX40-mediated memory T cell generation is TNF receptor-associated factor 2 dependent. *J. Immunol.* 171: 5997–6005.
51. Tafuri, A., A. Shahinian, F. Bladt, S. K. Yoshinaga, M. Jordana, A. Wakeham, L. M. Boucher, D. Bouchard, V. S. Chan, G. Duncan, et al. 2001. ICOS is essential for effective T-helper-cell responses. *Nature* 409: 105–109.